Design of an Automated Guided Vehicle for Material Handling

Maria Margarida Malveiro Bento das Dores Cheira
maria.cheira@tecnico.ulisboa.pt

Instituto Superior Técnico, Universidade de Lisboa, Portugal

July 2019

Abstract

This project is focused on the design of an automated guided vehicle (AGV) for material handling, to be implemented at a workshop at TAP. The material handling is currently done manually with the aid of carts.

Based on a preliminary design done prior to this work and the current activity at the workshop, a first concept for a AGV that would tow the carts was drafted. Following this, an analysis of the current carts is done, and a mechanism is developed in order to allow the carts to distribute material autonomously, as well as adaptations are suggested in order to allow the AGV to attach to the carts. The loads to which the AGV and the cart are subjected are then analysed and calculated by making assumptions about the dimensions of the AGV and then iterating on them. These allow for the calculation of the torque required for the AGV to pull the cart, which then allows for the dimensioning of the motor. It is also verified whether the AGV has enough traction to be able to pull the cart without slipping. Finally, a structural analysis is performed through a computational simulation to predict whether or not the structure of the AGV can withstand the loads previously calculated without yielding or disassembling.

Keywords: Material handling, Automated Guided Vehicle, Rolling resistance, Design, Finite element analysis

1. Introduction

When talking about the tasks of intralogistics in industrial environments, material handling appears as one the most important, as it heavily impacts the efficiency of the production process and its potential profitability [1]. The classical method used by companies was manual material handling, but, nowadays, the increasing trend has been the use of Automated Guided Vehicles (AGV). An AGV, as the name might imply, is a vehicle that doesn't rely on a human driver.

While replacing a human with a robot might have some drawbacks, namely the decreased flexibility and the high initial investment, it has been shown that AGVs reduce labour costs, improve safety conditions, and contribute to increased productivity [2].

The purpose of this project is to design an AGV to be introduced at the hydraulic and pneumatic (HP) workshop at TAP.

2. Theoretical Background

In order to begin modelling an electric vehicle, it's important to understand the relationship between the motion the vehicle is required to generate and the forces that it will be subjected to. The typical forces a vehicle will usually have to overcome are the ones described in the following subsections.

2.1. Rolling Resistance

Rolling resistance (F_{rr}) results from the deformation of a wheel against the ground. Because the material of the wheel isn't perfectly elastic, as the wheel turns there will be energy losses. Translating this to forces, it means that the force distribution in the contact area will not be even [3], and the resulting normal reaction will be misaligned with the centre of the wheel, as can be seen in Figure 1.

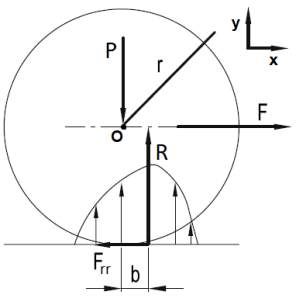

Figure 1: Forces acting on a wheel being pulled (adapted from [3])

Applying the dynamic equations of motion one gets:

$$\sum F_x = m_{wheel}a = F - F_{rr} \quad (1)$$

$$\sum M_0 = I\alpha = F_{rr}r - Rb \Leftrightarrow F_{rr} = I\frac{a}{r^2} + \mu_{rr}R \quad (2)$$

where m_{wheel} is the mass of the wheel, a is the acceleration, r is the radius of the wheel, b is the horizontal distance between R and the centre of the wheel, P is the vertical load on the wheel including weight, R is the normal reaction, F is the force pulling the wheel, I is the moment of inertia of the wheel, $\alpha = \frac{a}{r}$ is the angular acceleration of the wheel, and $\mu_{rr} = \frac{b}{r}$ is the rolling friction coefficient.

2.2. Aerodynamic Drag

Drag is the force that a fluid will exert on a moving body that is opposite to its relative motion. Aerodynamic drag (F_{ad}) is the term used when the surrounding fluid is air, and it can be expressed by equation (3),

$$F_{ad} = \frac{1}{2}\rho_{air}v^2C_DA \quad (3)$$

where ρ_{air} is the air density, v is the relative speed between fluid and body, C_D is the drag coefficient, and A is the characteristic area.

2.3. Force of Gravity on an Inclined Plane

When a vehicle is moving on a plane with inclination ψ, its weight (W) is going to have a component that is normal to the ground and another that is parallel. Only the component parallel to the ground will oppose the movement, and can be defined as:

$$F_{slope} = Wsin\psi \quad (4)$$

2.4. Tractive Effort and relation with Torque

The force that will propel the vehicle forward is typically called the tractive effort (F_{te}) [4], and must be able to overcome all the forces that were described above, as well as external forces that may be acting on the vehicle in the direction of motion($F_{ext,x}$). As such, the tractive effort can be defined by equation 5.

$$F_{te} = m_{vehicle}a + F_{rr} + F_{ad} + F_{slope} + \sum F_{ext,x} \quad (5)$$

This force is the result of the static friction that occurs between the wheel and the ground as a result from a torque being applied to the wheel by a motor. The free body diagram of a motorized wheel pulling a load can be seen in Figure 2.

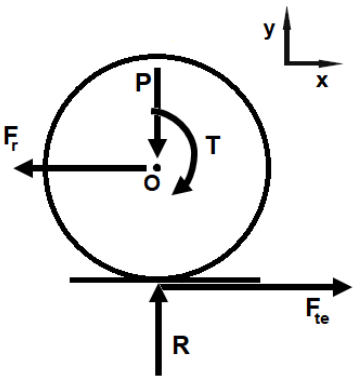

Figure 2: Free body diagram of a motorized wheel.

Applying the dynamic equations of motion results:

$$\sum F_x = m_{wheel}a = F_{te} - F_r \Leftrightarrow F_r = F_{te} - m_{wheel}a \quad (6)$$

$$\sum M_0 = I\frac{a}{r} = T - F_{te}r \Leftrightarrow T = F_{te}r + I\frac{a}{r} \quad (7)$$

where F_r is the load being pulled, and T is the torque.

3. Project Framework

3.1. Workspace and Current Activity

The workshop where the AGV will be introduced is divided into several groups, each dedicated to a different category of part or type of repair. Due to constraints regarding the layout of the workshop, this work will be focused on only four main groups, two on each side of a 5 meter wide corridor.

Each day, parts are delivered at the reception/expedition (RE) area in need of repair or maintenance. There, workers separate the parts into trays according to which group they are meant to be delivered to. A worker will then deliver the trays with the aid of a cart, as seen in Figure 3.

In each group there are two separate but similar stations containing shelves: a reception station, where the worker places the trays with the unrepaired parts, and an expedition station, where the worker takes the trays with the repaired parts from. The trays with the repaired parts are then taken back to the RE area.

3.2. Requirements and Restrictions

The AGV must be able to follow a defined path, know when to stop, and be able to recognize obstacles and avoid bumping into them. It should also be able to transport, pick up, and deliver material throughout the different work groups. It should be able to do all of this autonomously. It should be designed so that it can be built using TechnoLean

Figure 3: Cart with trays

material from the company Quimilock, since this type of material is readily available at TAP, and preferably it should be made the most use out of what already exists at the workshop. Also, the introduction of the AGV in the workshop should not interfere (or the interference should be minimized) with the current mode of operation in the workshop. In terms of battery life, the AGV should be able to work a full shift, but should also have an autonomous charging scheme, and should be able to take any opportunity to charge the battery.

While a budget was not defined for the designed of the AGV, an effort should be made in keeping the design simple and affordable.

3.3. Previous Work

The introduction of an AGV on this particular workshop at TAP is a project that has already seen some study. Prior to this work, Enrique Serrano Martínez [5] wrote a thesis where a preliminary design for the AGV's system was made. In it, he concluded the best type of AGV for this workshop would be an underride AGV, with a lifting table to lift the carts, that would follow a magnetic tape around a path like the one seen in Figure 4.

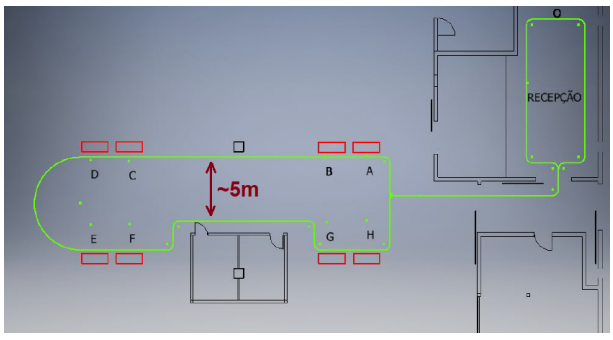

Figure 4: Single loop path with a single unidirectional lane [5]

The AGV would also have a tricycle configuration, meaning it would have a steerable drive wheel at the front and two supporting wheels at the back. The motorized wheel chosen for this application was the one by the Italian company C.F.R..

For this type of vehicle, the use of rechargeable batteries was more convenient. It was decided that lithium-ion batteries would be used, since they don't have memory effect, the AGV can take advantage of idle time to charge, and not just when the battery is fully drained.

Table 1 displays the estimated final dimensions of the AGV, as well as the weight.

Table 1: Vehicle total dimensions

Length (mm)	1875
Width (mm)	600
Height (mm)	294
Weight (kg)	172.05

One of the main downsides of the preliminary design was the fact the the vehicle was very long. The carts that the AGV is supposed to carry are 920 mm long, making the AGV almost a full meter longer than its cargo. However, the preliminary design was completely restrained by the dimensions of its components, namely the lifting table, which was the biggest component in the AGV. The decision was thus made to change the type of AGV from a lifting underride to a towing underride.

4. Material Distribution System

4.1. Current Carts and Cargo

A schematic of the carts being currently used can be seen in Figure 5, and a picture has been shown previously in Figure 3.

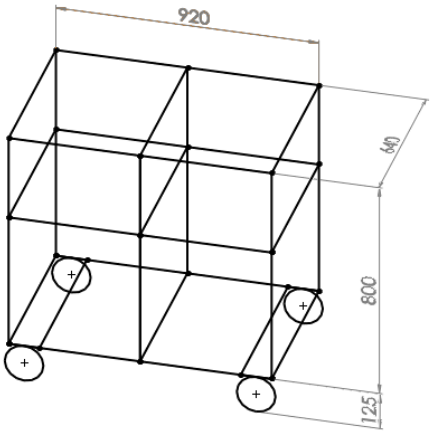

Figure 5: Cart measurements in mm

The carts were built using only TechnoLean material, and consist of a combination of tubes connected by joints, all made of steel. They are supported by four swivel castors connected to corner

plates. The carts have two levels of shelves, with two shelves each. Each shelf can fit one 600x400 mm tray or combinations of smaller trays. The shelves of the carts are composed of inclined roller tracks that are limited laterally by descend guides. This inclination is of about is of about 3° and is achieved through the use of connectors with different heights. These connectors don't allow the trays to slide off the shelf.

The maximum total weight of the cart plus cargo was estimated to be of approximately 108 kg.

The aforementioned expedition and reception stations have a structure similar to the carts, in the sense that they also have inclined shelves composed of roller tracks, where the shelves from the reception station are inclined away from the corridor, so that the trays slide in the direction of the work area, and the expedition station's shelves are inclined towards the corridor. Their placement in the workshop and relatively to the path of the AGV can be seen in Figure 4, where A, C, E, and G are reception stations, and B, D, F, and H expedition stations. The path of the AGV will thus follow along the stations from A to H, and it can be seen the stations will be to the right of the AGV as it passes by them.

4.2. Distribution System

In order for the automatic distribution to be made possible, the trays need to be able to slide off the shelves and onto the reception stations. This can be achieved easily through a change in the connectors that secure the roller tracks.

The cart should thus approach the reception station, moving parallel to it, and stop in front of it, so that the shelves of the cart align with the shelves of the station. The trays should then slide from the side of the cart to the reception station's shelves, as can be seen schematically represented in Figures 6 and 7.

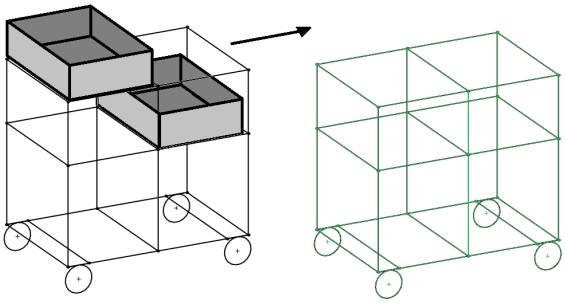

Figure 6: Cart approaching

Now, a solution to control the sliding of the trays was necessary. After some research, one by the company item was found, which can be seen in Figures 8 and 9.

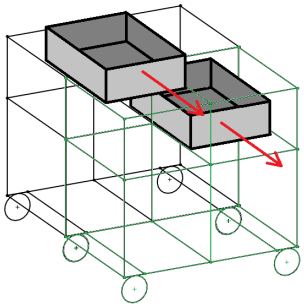

Figure 7: Tray delivery.

Simply explained, this mechanism consists of a number of stoppers that prevent the tray from sliding off the inclined shelf. The stoppers can rotate around an axis and are connected to a bar that has a protruding roller. When the cart approaches the receiving shelf, the roller will come into contact with a ramp, forcing the stoppers to rotate and allowing the tray to slide freely. The stoppers are then brought back to their original position by a spring.

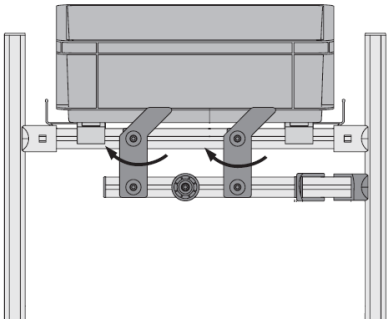

Figure 8: Schematics of item mechanism – closed setting [6]

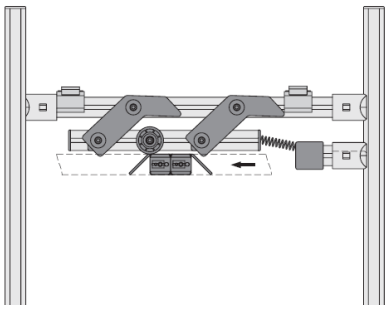

Figure 9: Schematics of item mechanism – open setting [6]

An attempt was made to recreate this mechanism

using TechnoLean material. The result, which will henceforth be referred to as lock, can be seen in Figure 10.

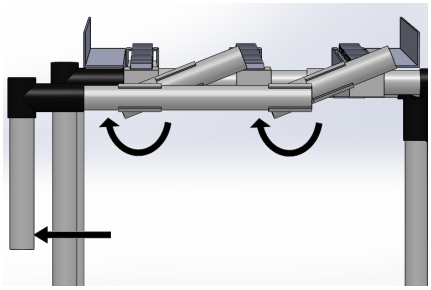

Figure 10: Lock – open setting

This mechanism uses four rotating connectors, and two parts forming a 'T' joint. As for the roller (not represented in the figures), one possible option would be to use a wheel that is used for the roller tracks.

Because this lock is completely mechanic, it was necessary to ensure that each tray would only be released at the right time, i.e., that each of the cart's shelves would only be triggered to open by the correct receiving shelf, and no other. The most versatile solution achieved would be to place ramps at different heights in each station and make the rollers adjustable in height, so that every shelf could potentially serve every station. For example, this would cover both the possibility of there being a tray to deliver to each station or all trays to one station alone, just by adjusting the height of the rollers, as seen in Figure 11 (for the sake of clarity, the schematics from item were made use of for the picturing of this solution).

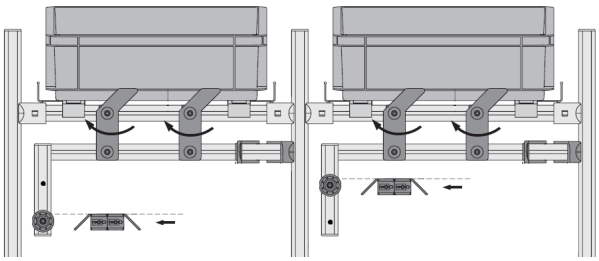

Figure 11: Adjustable rollers (adapted from [6])

Since this solution would allow for the possibility of all shelves carrying trays to one single group, then the receiving shelves should be made compatible with the cart, having the same two levels with two shelves each.

4.2.1 Potential Conflicts and Resolution Suggestions

The last solution suggested implies that the vertical arm of the lock should have four different height settings for the roller, one for each group. However, for two shelves at the same level, if the rollers were placed on the same setting, those shelves would be activated more than once, which could lead to a tray being delivered to the wrong place.

One possible solution would be to add a vertical offset to misalign the levels of the rollers for same level locks, as shown in Figure 12.

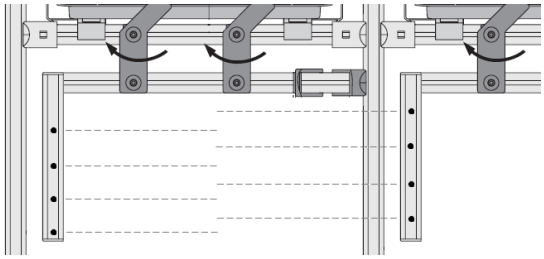

Figure 12: Vertical misalignment (adapted from [6])

This could also be achieved with a horizontal offset, in which the roller levels would still be aligned vertically, but on the locks from the cart's rear shelves, the rollers' notches would be more protruding than the aft shelves, and their corresponding activating ramps should be receded, so that they only activate the locks of the rear shelves. A schematic can be seen in Figures 14 and 13.

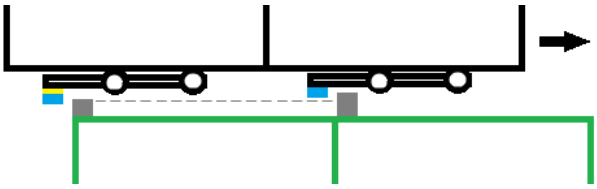

Figure 13: Schematic view from above. The reception shelves are represented in green, the ramps in grey, the rollers in blue, and the offset in yellow.

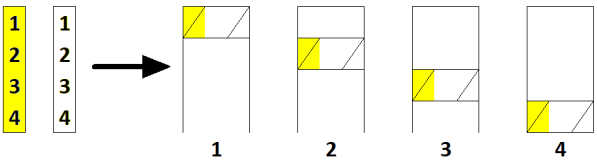

Figure 14: Horizontal misalignment. The yellow shaded areas represent the rollers and ramps that have an offset, and the arrow represents the direction of motion of the cart

In Figure 14, the vertical rectangles on the left

represent the two locks and the four different levels for the rollers, and the numbers represent each of the groups. On the right are represented the groups' reception stations, where the diagonal lines represent the activating ramps.

4.3. Expedition System

Besides delivering trays, the AGV is also expected to aid in retrieving trays containing repaired parts.

As was explained before, both the reception and expedition stations will be to the right of the AGV, and it was also mentioned that what differentiates them is the direction to which their shelves are inclined. The cart, however, will have all the shelves inclined the same way, so for it to be able to receive trays from the expedition stations, the cart would have to be turned around. Because this can't be done during a route, the reached solution requires the distribution of trays and the collection of trays to be done in separate routes.

In the routes where the AGV retrieves the repaired parts, the cart should thus be attached to the AGV in a backwards position, with the shelves descending to the left. The mechanism that allows the sliding of the trays from the stations' shelves to the cart would be the same as described before, using a combination of locks activated by ramps, but, in this case, the locks would be attached to the stations' shelves whereas the activating ramps would be on the cart.

Since there is no way of knowing a priori how many trays there are in each group ready to be collected, then the best way to avoid any conflicts is to reserve each shelf on the cart to a single group. This would mean that in each expedition station, only one shelf would be activated by the cart, rendering the other shelves useless from the perspective of the AGV.

One suggestion to counteract this problem would be to redesign the expedition shelves so that this single shelf would be automatically supplied with another tray whenever it was emptied by the AGV. Figure 15 shows the schematics for an example mechanism.

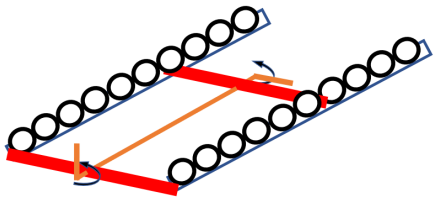

Figure 15: Example of mechanism for expedition shelves

Unfortunately, due to lack of time, it was not possible to further develop and concretize this solution, but it remained worth to mention, as it could be relevant for future developments.

4.4. Coupling

It was determined earlier that the AGV would transport the carts by means of a towing device. A similar project [7] accomplished this by means of a towing pin, which was activated with the help of a linear actuator.

Since the carts are supported by swivel castors, to avoid the cart and the AGV to rotate relative to each other during curves, potentially causing collisions between the AGV's and the cart's structures, it was concluded that the use of two pins would be better than just one.

Figure 16 portrays the suggested design of the coupling structure.

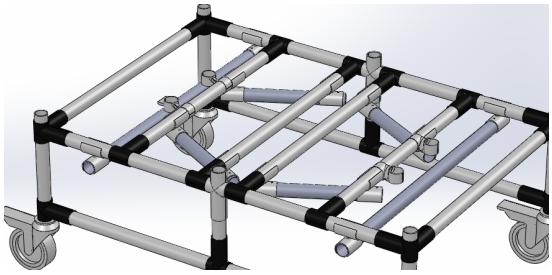

Figure 16: Coupling structure (sectioned view)

As can be seen, the structure is symmetrical, so that the AGV can attach to the cart in both directions. The diagonal pieces that appear in the design should serve as guides for the towing pins, in case the cart is placed slightly misaligned. At the end of those guides, there are two 90^o crossover tube joints, where the pins will hook on to. As can also be seen, the guides and the hooks are at different heights, meaning that instead of a linear actuator, it will likely be necessary a linear servo to control the height of the pin.

The general look of the final design of the cart can be seen in Figure 17.

5. Designing the AGV

5.1. Equations of Motion

As was explained in Section 2, to model an electric vehicle one must know how its motion relates to the forces that it's going to be subjected to. In that section, equation (5) was defined as a general equation that describes just that. It is now imperative to apply and further expand that equation so as to fit the specific case of this project.

Figures 18 and 19 display the free body diagrams of the AGV and the cart, respectively, where F_1 is the tractive effort, F_2 and F_4 are the rolling resistance of each individual pulled wheel, F_3 is the

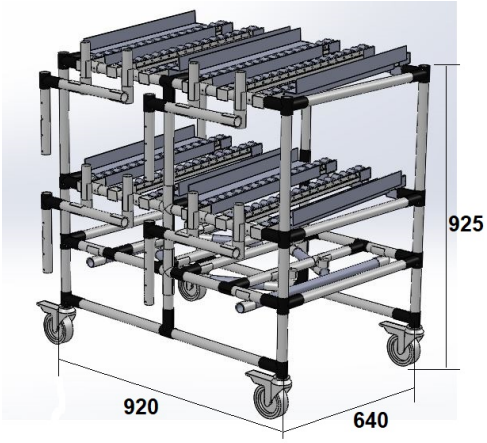

Figure 17: 3D drawing of the cart (dimensions in mm)

force pulling the cart, $W_{AGV} = m_{AGV}g$ is the total weight of the AGV, $W_{cart} = m_{cart}g$ is the total weight of the cart, L_x is the horizontal distance between front wheel and center of gravity of the AGV, L_y is the vertical distance between F_3 and the ground, and l is the horizontal distance between front wheel and back wheels of the AGV.

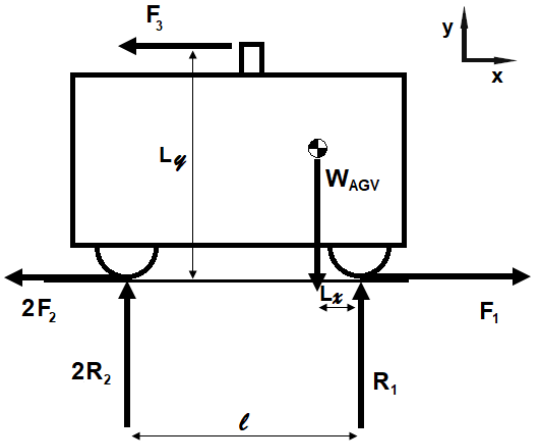

Figure 18: Free body diagram of the AGV

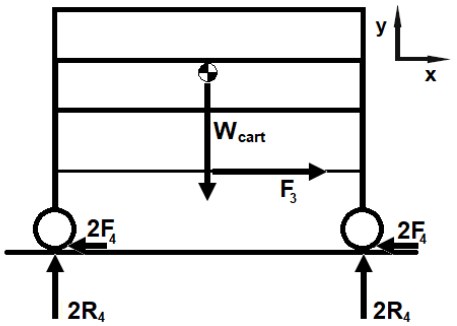

Figure 19: Free body diagram of the cart

For the case of this project, the aerodynamic drag and the slope were disregarded. This is because the ground is plane all throughout the workshop, so the AGV is not expected to encounter any slopes. Besides this, the AGV will not move at great speed, so the aerodynamic drag will be very small in comparison to the rest of the forces.

Applying the equations from Section 2, results the system of equations (8), which defines the kinetics of the AGV.

$$\begin{cases} R_4 = \frac{W_{cart}}{4} \\ F_4 = I_4 \frac{a}{r_4^2} + \mu_{rr,4} R_4 \\ F_3 = m_{cart} a + 4F_4 \\ R_2 = \frac{F_3 y + W_{AGV} x}{2l} \\ R_1 = W_{AGV} - 2R_2 \\ F_2 = I_2 \frac{a}{r_2^2} + \mu_{rr,2} R_2 \\ F_1 = m_{AGV} a + 2F_2 + F_3 \end{cases} \tag{8}$$

5.2. First Design Iteration

In order to solve (8), some values need to be defined or assumed.

Previously in Section 4.1, it was defined that the maximum weight of the cart plus the cargo would be of around 108 kg.

The cart's wheels and the AGV's back wheels are both swivel castors with rubber wheels of similar mass and radius, meaning their moments of inertia will be the same. The radius of the wheels is 50 mm and its mass was assumed to be approximately 0.5 kg. To simplify, it'll be assumed their moment of inertia is approximately the one of a solid cylinder.

$$I_2 = I_4 = \frac{1}{2} m_{wheel} r_{wheel}^2 = 0.000625 \ \ kg \cdot m^2 \tag{9}$$

As for the weight of the AGV, a first estimate of 75 kg was considered.

In terms of acceleration, since the AGV isn't going to achieve high speeds (about 1.4 m/s), there's no need for a very high acceleration, so an acceleration of 1 m/s^2 was assumed.

Dimensions L_x, L_y and l were defined as 0.2 m, 0.3 m, and 0.9 m, respectively.

The values of $\mu_{rr,2}$ and $\mu_{rr,4}$ were calculated using equations (10) and (11), which were derived from an equation by I. Evans [8] for solid rubber tyres, assuming a rigid ground.

$$\mu_{rr,2} = \frac{h}{4.4} \left(\frac{R_2 t}{E s r^2} \right)^{\frac{1}{3}} \tag{10}$$

$$\mu_{rr,4} = \frac{h}{4.4} \left(\frac{R_4 t}{E s r^2} \right)^{\frac{1}{3}} \tag{11}$$

where h is the fraction of energy dissipated, t is the thickness of the tyre, E is the modulus of elasticity

of the tyre, s is the width of the wheel, and r is the radius of the wheel.

From taking measurements of the wheels, it is known that t =7.5 mm, s =32 mm, and r = 50 mm, and a modulus of elasticity of 0.001 GPa was used to calculate the rolling friction coefficients. The h used was of 0.5.

With this, it is now possible to solve system (8) for all its variables. The results can be seen in Table 2.

Table 2: First iteration results

R_4 (N)	$\mu_{rr,4}$	F_4 (N)	F_3 (N)	R_2 (N)
264.87	0.033	8.99	143.96	105.74
R_1 (N)	$\mu_{rr,2}$	F_2 (N)	F_1 (N)	
524.27	0.024	2.79	224.54	

Having been calculated the tractive effort (F_1), it is now possible to calculate the corresponding necessary torque. The relationship between these two has been previously defined by equation (7).

The company C.F.R. was then contacted to ask about a motor that would be more appropriate for this project, and the model MRT05.D0101 was suggested. Table 3 shows a summary of the most relevant specifications.

Table 3: New steerable drive wheel information

Max. wheel torque (Nm)	180
Nominal wheel torque (Nm)	29.5
Wheel diameter (mm)	198
Material	Polyurethane
Total weight (kg)	42

From Table 3 we know that the wheel has a diameter of 198 mm, but no information is given about how much it weighs by itself, so an estimate was made of 5 kg. Assuming once again the moment of inertia of the wheel to be approximately the one of a solid cylinder, and applying equation (7) resulted a torque of 22.48 Nm. Seeing that in normal conditions the motor can continuously output a torque of 29.5 Nm, this gives a safety factor of 1.3.

As for the batteries, PowerBrick batteries by company PowerTech were considered. The batteries' specifications can be consulted in Table 4.

Table 4: Lithium Ion battery 12V 70Ah – LiFePO4 – PowerBrick specifications

Voltage	Capacity	Weight
12 V	70 Ah	9.8 kg
Energy	Dimensions L x W x H	
896 Wh	228 x 138 x 210 mm	

Connecting the batteries in series gives a total battery capacity of 140 Ah, which should allow a run time of approximately 6 hours.

5.3. 3D sketch of the AGV

Having in mind all of the previous considerations, a 3D sketch of the AGV was made to get a better idea of what the real dimensions of the AGV would resemble. The result can be seen in Figure 20.

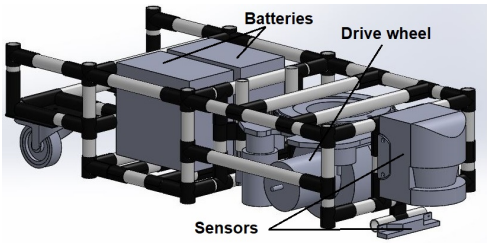

Figure 20: 3D drawing of the AGV

5.4. Second Design Iteration

Having accomplished a design for the AGV allows for new values that were previously assumed to be corrected.

For starters, taking into account the structure of the AGV is made of steel, and considering a typical value of 7900 kg/m^3 for its density, SolidWorks calculated that the weight of the structure would be of approximately 25 kg. Considering the rest of the main components amounted to a total weight of 92.15 kg. Using SolidWorks, it was also possible to determine the position of the center of mass of the structure. With this information, a new value for L_x of 0.176 m was determined, as well as a value for l of 0.758 m, and L_y was also measured to be approximately 0.32 m. Table 5 shows the new results obtained using the new values.

Table 5: Second iteration results

R_4 (N)	$\mu_{rr,4}$	F_4 (N)	F_3 (N)	R_2 (N)
264.87	0.033	8.99	143.96	135.34
R_1 (N)	$\mu_{rr,2}$	F_2 (N)	F_1 (N)	
633.31	0.027	3.90	243.91	

Applying equation 7, once again, results in a new value for the necessary torque of 24.39 Nm. This brings down the safety factor from the previously calculated 1.3 to 1.2. However, it's worth to note that the safety factor is being calculated in relation to the torque the motor can provide continuously, since, as seen in Table 3, the motor can output a maximum of 180 Nm before stalling. With a maximum speed of 1.4 m/s and an acceleration of 1 m/s^2, the AGV isn't expected to have to accelerate for more than 1.4 seconds at a time, so even if the output torque surpasses 29.5 Nm, this shouldn't

pose a problem to the motor.

5.4.1 Traction of the Motorized Wheel

While the motor may be powerful enough to provide the necessary torque, it's important to check if the motorized wheel has enough traction to the floor, so that it doesn't slip when it begins to roll. Slippage between two materials happens when the force used to drag an object through another exceeds the maximum static friction force, given by equation (12), where μ_s is the static friction coefficient between those two materials and R is the normal reaction.

$$F_{sf} = \mu_s R \tag{12}$$

In this case, the normal reaction is the last calculated R_1. The floor on the workshop is concrete and the material of the tyre of the wheel is polyurethane. A value of $\mu_s = 0.6$ between polyurethane and concrete was used. This results in a maximum static friction force of 380 N. Since this value is bigger than the 243.91 N calculated for the tractive effort, it can thus be concluded that the wheel will not slip.

6. Structural Analysis

Having the design been made and the loads involved analysed and calculated, it is now necessary to make sure that the structure of the AGV can withstand such loads through a structural analysis.

The material used to design both the cart and the AGV is comprised of steel tubes connected by steel joints. The tubes have a 28.6 mm outer diameter and have a thermoplastic coating. The coating has a 0.8 mm thickness, and covers a steel tube of 27 mm outer diameter, which can have 1 mm (T1) or 2 mm (T2) thickness.

The company provided the information that the steel was a E260 type steel. The properties of this material can be found in Table 6.

Table 6: Mechanical properties for E260 steel [9]

Young's Modulus (GPa)	190
Poisson's Ratio	0.29
Yield Strength (MPa)	290

As for the joints, the TechnoLean catalogue [9] states that they can endure a load of 100 kg being applied to a tube axially or transversally before the joint is separated from the tube or slides across one.

6.1. Finite Element Analysis

Finite element analysis (FEA) is a computational analysis that uses the finite element method (FEM), which is a numerical method of approaching an engineering problem. The basic idea behind it is that it takes a given geometry and divides it into smaller pieces, called finite elements, over each of which an algebraic equation that is compatible with the neighbouring elements is derived. These equations are then solved simultaneously to obtain the solution to the problem as a whole [10]. The finite elements connect to each other through nodes. Together, the elements and the nodes form a mesh in the shape of the initial geometry. Creating the mesh is a pivotal step of the FEA, as the quality of the results generated correlates directly with the quality of the mesh [11].

Because the structure is composed of tubes of constant section and material, 1D elements of type CBAR were deemed appropriate for this analysis, and some RBE2 elements were used to simulate contact between some tubes.

For this project it was used the Siemens NX software.

6.1.1 Modelling the Geometry

When modelling, all the tubes were defined as T1 tubes, the purpose being to check if there were any tubes that needed reinforcement and required to be replaced by thicker tubes. The meshed geometry can be seen in Figure 21.

The loads were applied so as to represent the weight of the structure itself, as well as the weight of the components of the AGV, and the force representing the pulling of the cart. The weights of the wheels were not represented seeing as the structure will be supported by them, and not exactly be under the effect of their weight. Instead, the wheels were represented by the constraints, represented in orange in Figure 21. The way the constraints were represented were that, for the motorized wheel, the structure was fixed in four points at approximately the positions where the drive wheel would be bolted to the tubes, and the back wheels were represented by two simply supported constraints.

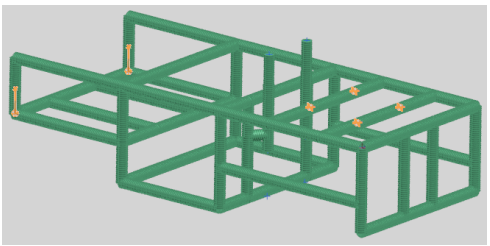

Figure 21: Meshed geometry with constraints (in orange)

6.1.2 Analysis and Results

A linear static analysis was then performed. A linear static analysis is one where the material follows a linear elastic behaviour and the forces aren't varying with time, and small displacements are assumed [11]. This analysis outputs the stress state

and displacements of the structure for the prescribed loading and constraints.

A mesh convergence study was performed to ensure the quality of the mesh, and the results were taken when convergence was achieved.

The analysis showed that the maximum von Mises stress reached was of 15.81 MPa. The von Mises yield criterion states that a material will yield when its stresses reach the value of the yield strength of that material. The yield strength of the steel of the tubes is of 290 MPa (refer to Table 6), meaning the loads are not likely to cause the structure of the AGV to yield. The shear forces and the axial force can be compared to the joint strength given by the company, which was of 100 kg (981 N). The maximum shear force and axial force registered was of 135.38 N and 77.72 N, respectively, which are much inferior to 981 N, meaning there is also very little risk of the joints separating or sliding.

7. Conclusions

In this work, a functional concept for the material distribution mechanism was achieved, as well as a design for the AGV.

It was concluded that the current carts used at the workshop need adaptations in order to be made compatible with an AGV, but those adaptations are very minor and should not impact the structural soundness of the cart when it comes to carrying material. Calculations performed allowed to determine the loads to which the structure of the AGV would be subjected to, and two iterations were performed to achieve the final results and a final design that should be able to pull a fully loaded cart without slipping.

As for the structural analysis, the FEA showed that the structure of the AGV should withstand the loads it will be subjected to without yielding and without causing separation of joints.

7.1. Future Work

It is paramount that a further study be made into the electronic components that would be required and adequate to be used on this project, as well its circuit design, and also the construction of a prototype. It is also necessary to create an algorithm for the operation and do the programming and control of the AGV, and to create a user friendly platform to be used by the workers at the workshop to instruct the AGV, and create schedules and routes for it. It would also be advisable to look into the usage of sensors on the carts and/or on the reception and expedition stations to be used as extra safety measures and ensure the correct delivery of trays.

References

[1] G. Ullrich. *Automated Guided Vehicle Systems: A Primer with Practical Applications*. Springer-Verlag Berlin Heidelberg, 1^{st} edition, 2015. ISBN 978-3-662-44813-7.

[2] Conveyco. The Advantages and Disadvantages of Automated Guided Vehicles (AGVs). https://www.conveyco.com/advantages-disadvantages-automated-guided-vehicles-agvs/. Accessed: 02-05-2019.

[3] Elesa Ganter. Castors and Wheels. https://www.elesa-ganter.com/static/technicaldata/files/Castors_and_Wheels_TD_EN.pdf. Accessed: 01-04-2019.

[4] J. Larminie and J. Lowry. *Electric Vehicle Technology Explained*. John Wiley & Sons Ltd, 1^{st} edition, 2003. ISBN 0-470-85163-5.

[5] E. S. Martínez. Preliminary Design of an Automated Guided Vehicle (AGV) System. Master's thesis, Instituto Superior Técnico, 2018.

[6] item. Release Unit D30 Bar T1. https://product.item24.de/en/products/product-catalogue/productdetails/products/low-cost-automation-the-mechanical-solution-1001390644/release-unit-d30-bar-t1-65884/. Accessed: 15-04-2019.

[7] T. P. Ferreira and I. A. Gorlach. Development of an affordable automated guided cart for material handling tasks. *International Journal of Circuits and Electronics*, 1, 2016. ISSN: 2367-8879.

[8] I. Evans. The rolling resistance of a wheel with a solid rubber tyre. *British Journal of Applied Physics*, 5(5):187–188, March 1954.

[9] Technolean. Components Catalogue. https://www.technolean.com/wp-content/uploads/2018/12/181212_Technolean_Catalogo_ENG-web.pdf. Accessed: 30-04-2019.

[10] J. N. Reddy. *An Introduction to the Finite Element Method*. McGraw-Hill, 3^{rd} edition, 2006. ISBN 007-124473-5.

[11] *Practical Aspects of Finite Element Simulation - A Study Guide*. Altair University, 3^{rd} edition, 2015.